Journal of Oil Palm Research Vol. 38 (1) March 2026 p. 174–189
DOI: https://doi.org/10.21894/jopr.2025.0006

DELVING INTO THE SYNERGISTIC BEHAVIOURS OF TRIBOLOGICAL ADDITIVES IN MINERAL AND VEGETABLE OILS VIA THERMODYNAMIC ANALYSIS

CHUNG-HUNG CHAN[1]*; AHMAD SYAFIQ AHMAD HAZMI[1]; NOOR KHAIRIN MOHD[1]; WEN HUEI LIM[1] and SIN YEE GAN[1]

ABSTRACT

This study presents a comprehensive thermodynamic modelling and analysis to enhance lubrication assessment in tribotests, focusing on ASTM D2783 extreme pressure (EP) and ASTM D4172 anti-wear (AW) tests. The model facilitates the identification of optimal high-performance lubrication and synergistic additive combinations, even for lubricants yielding similar test results. A case study evaluates 36 lubricant samples, including mineral oil, vegetable oil, and blends. Rooted in the entropy balance, the model employs the dissipative coefficient U_w *to simulate friction-wear interplay, providing insights into wear conditions, lubrication mechanisms and efficacy. Both mineral-based and vegetable-based lubricants exhibit analogous friction-wear dynamics, but their compatibility with additives differs, resulting in distinct synergistic packages. Blended base oils' compositional complexity significantly influences additive synergies, challenging conventional tribotest evaluations. The* U_w *parameter-based approach empowers the selection of optimal lubricant formulations, aiding in designing effective lubricant solutions by considering wear conditions, lubrication mechanisms, and additive compatibilities.*

Keywords: additive, entropy dissipation, formulation, friction, lubricant.

Received: 16 February 2024; **Accepted:** 24 October 2024**; Published online:** 19 February 2025.

INTRODUCTION

Palm oil stands out as the most extensively utilised vegetable oil globally, contributing to about 40% of the total production of all vegetable oils combined (Gan et al., 2023). This places palm oil at the forefront as a promising candidate for use as a biolubricant base stock. According to Lee et al. (2022), palm is the most studied bio-lubricant, followed by castor oil. Its substantial production establishes its significance in the food market and as a commodity and positions it as a viable alternative in the biolubricant sector, offering the potential to replace traditional petroleum-based lubricants (Parveez et al., 2023). Biolubricants derived from renewable resources are generally perceived as environmentally friendly, biodegradable and non-toxic lubricants. Biolubricant products can be made up of blending through either partially or completely with bio-based oil. This depends on the requirements of international standards such as bio-based content, biodegradability and technical performance. In general, lubricant formulation development involves multi-objective optimisation of the types and compositions of base stocks and additives. Among the additives, tribological additives are one of the important elements to ensure optimum lubrication performance such as anti-wear (AW) and load-carrying capabilities (Bart et al., 2013). The investigation of the tribological behaviours of the additives is crucial in lubricant formulation development. Such investigation is usually conducted through

[1] Malaysian Palm Oil Board,
6, Persiaran Institusi, Bandar Baru Bangi,
43000 Kajang, Selangor, Malaysia.

* *Corresponding author e-mail: rykenz87@yahoo.com, chan@mpob.gov.my*

a series of tribological assessments such as Four-ball tribo-testers and pin-on-disc tribo-tester. One of the flaws of these physical assessments is that they rely heavily on friction and wear parameters to assess lubrication performance, without considering the underlying fundamental mechanism of the sliding phenomenon in situ. As a result, the investigation of additives behaviours and synergy can be difficult and misleading if complex interaction of the additives is involved. Under these circumstances, a tribological model can be employed to support the tribological assessments.

Tribological modelling has evolved to support advancements in various applications, including lubrication, coating, and surface materials. Initially rooted in a basic contact mechanics approach, tribological modelling has progressed toward a more intricate multi-physical approach. This advanced approach encompasses different time scales, length scales, and conditional states, enhancing our understanding of tribological phenomena (Vakis et al., 2018). Indeed, tribological modelling plays a pivotal role in simulating and predicting the friction and wear behaviours of a tribology system. Traditionally, Reynolds Equation has been employed to analytically solve the classical lubricated contact problems considering the non-Newtonian effect, surface roughness effect (Allmaier et al., 2012), surface topography effect (Ripoll et al., 2011), thermal effect (Li et al., 2013; Ouyang et al., 2017), and boundary lubrication behaviours (Mukchortov et al., 2017). The capabilities mentioned above necessitate the integration of additional model frameworks (e.g., asperity contact model [Ripoll et al., 2011]) and advanced approaches (e.g., finite element method contacts [Hao & Meng, 2015; Ripoll et al., 2011]), molecular dynamic simulation (Ghaffari et al., 2018; Godlevskiy & Blinov, 2016), making them highly complex and tend to require long computational time. In addition to the Reynolds Equation and its variants, other lubrication models revolve around regression analysis based on statistical approaches (Baskar et al., 2016; Simonovic & Kalin, 2016; Weinebeck et al., 2017; Xiong et al., 2015), empirical model driven by experimental observations (Hu et al., 2017; Zhou et al., 2018), and models derived from first principles (Chong & Ng, 2016; Ghanbarzadeh et al., 2016; Lyashenko & Khomenko, 2012). Typically, these models offer "black box" simulations, where the intricacies of the contact phenomena are obscured or not fully captured.

Conversely, wear modelling typically follows friction and lubrication modelling in sequence (Gao et al., 2018; Li & Anisetti, 2017; Zhang et al., 2017), although it can be conducted independently provided that information on asperity contacts (or models), the mechanical properties of the surfaces, the wear mechanism, and the lubricant actions are known (Bosman & Schipper, 2011, 2012; Mishina & Hase, 2013). Due to the limited and incomplete understanding of wear mechanisms, even at the macroscopic level, wear modelling is primarily conducted using empirical approaches (Cao et al., 2015; Gao et al., 2018; Mishina & Hase, 2013; Tan et al., 2015; Zhang et al., 2017). Considering the aforementioned models, it's evident that most friction and wear models were developed for very specific systems, lacking the desired level of generality (Banjac et al., 2014). Undoubtedly, these models are useful for describing specific phenomena in tribology. However, there remains a lack of clarity and connection between friction and wear, as their mutual dependence and correlation among themselves are often unclear and disconnected (Banjac et al., 2014).

The correlation between the friction and the wear behaviours of a tribological system is possible to be established through thermodynamic analysis and modelling. In this model, the tribological system can be seen as a thermodynamic system that deteriorates irreversibly with the dissipation of energy (Abdel-Aal, 2010; Amiri & Khonsari, 2010; Fox-Rabinovich et al., 2007; Gershman et al., 2016; Ramalho & Miranda, 2006). This work demonstrated a method to assess and evaluate the synergistic behaviours of tribological additives in lubricants using thermodynamic analysis to further extend its use. The interaction of different additives in lubricant formulation is crucial to be investigated as it creates synergistic or antagonistic effects. Some synergistic effects are difficult to observe as the interactions are specific and only happen at certain contact conditions (Tomala et al., 2017; Yang et al., 2021) and temperature (Yang et al., 2021). For instance, the presence of zinc dialkyldithiophosphates (ZDDP) additive in PAO enhances the friction-reducing and AW effect of WS2 nanoparticles in the boundary lubrication regime (Aldana et al., 2016).

In this study, thermodynamic analysis is performed on Four-ball lubrication to map the friction-wear relationship of the lubrication. The mapping is then used to assess and evaluate the additive synergy of 36 lubricant samples comprising vegetable oil, mineral oil and their blends formulated with several AW and extreme pressure (EP) additives. Besides, the effect of different base oils (BASE) on the additive compatibility in the formulation is also investigated. Finally, an empirical approach to select the best lubricant formulations from the thermodynamic viewpoint is developed and demonstrated.

MATERIALS AND METHODS

Materials and Reagents

Mineral oil (M) i.e., G2 SN150 from H&R (Malaysia) Sdn. Bhd., and vegetable oil (V), i.e., palm olein from the local market were used as the BASE in this study. Two commercial AW additives (A1 and A2) and one commercial EP additive (A3) were obtained from a local supplier. A1 is a multifunctional complex ester designed to enhance lubricity, reduce wear, and prevent corrosion in milky, semisynthetic, and neat oil metalworking fluids. A2 is a high molecular weight polar polymer equipped with various functional groups, used to improve lubricity in rolling emulsions and in cutting and forming fluids. A3 is a sophisticated compound frequently used to boost the EP capabilities of working fluids, suitable for both ferrous metals and aluminium alloys.

Lubricant Formulations

In this study, 36 lubricant samples were prepared according to the following formulations in the format of BASE either M, V, or their blends together with additives (A1, A2, A3) as tabulated in *Table 1*.

TABLE 1. LUBRICANT SAMPLES FORMULATION

No.	Formulation of lubricant
1	BASE
2	BASE + A1 (2% w/w)
3	BASE + A2 (2% w/w)
4	BASE + A3 (2% w/w)
5	BASE + A1 (2% w/w) + A3 (2% w/w)
6	BASE + A2 (2% w/w) + A3 (2% w/w)
	BASE in the formulation
1	M
2	80% v/v M + 20% v/v V (M80 + V20)
3	60% v/v M + 40% v/v V (M60 + V40)
4	40% v/v M + 60% v/v V (M40 + V60)
5	20% v/v M + 80% v/v V (M20 + V80)
6	V

Note: BASE - base oil; M - mineral oil; V - vegetable oil.

Tribological Testing

The tribological behaviours of the 36 samples were assessed using a Four-ball test machine (DUCOM TR-30, Ducom Instruments, USA). In this configuration, a steel ball is rotated against three stationary steel balls under specific load and speed conditions. The employed test methods are the ASTM D2783 EP test (ASTM International [ASTM], 2019) and the ASTM D4172 AW test (ASTM, 2020). Given the test method, the EP test assesses the ability of the lubricant to work under extreme load conditions such as in bearing application. The EP ability is commonly determined by the weld point, which is the load at which the sliding surfaces seize and then weld, or the stationary balls having wear scar diameter above 4 mm. The EP test is first evaluated at 80 kg load, 1,760 rpm rotation speed and 10 s sliding time, and then it is repeated at incremental loads till the weld point. On the other hand, the AW test measures the wear-preventive characteristics of the lubricant sample based on the wear scar diameter and the average friction coefficient. This test is conducted at a load of 40 kg, rotation speed of 1,200 rpm and time of 3,600 s.

Thermodynamic Analysis

The EP and AW test results were analysed via the thermodynamic modelling framework obtained from our previous work (Chan et al., 2020). In the modelling framework, the rate of entropy generation due to friction from the sliding (or rotating activity) of the tribosystem can be expressed as Equation (1):

$$\frac{dS_i}{dt} = \frac{(\mu w v)^2}{A_c U T^2} \quad (1)$$

where, dS_i is the entropy production due to frictional sliding; μ is the friction coefficient; w is the normal load; v is the sliding speed; U is the heat transfer coefficient of the domain; A_c is the interfacial contact area; t is the time domain, and T is the lubrication temperature. Naturally, certain entropy dissipation mechanisms occur within the tribosystem to counteract the effects of entropy generation due to friction, ensuring the prevalence of sliding activity. The first entropy dissipation mechanism considered in this study is the wearing process, as described in Equation (2):

$$\frac{dS_w}{dt} = \frac{2\gamma}{T}(b \times k_w w v) \quad (2)$$

where, dS_w is the decrease in entropy as a result of the wearing process, γ is the surface energy of the worn material, b is the ratio of worn surface area to the worn volume, k_w is the specific wear rate (total wear volume divided by load and sliding distance). The ratio b depends entirely on the geometry of contact (e.g., flat-on-flat, ball-on-flat). Another entropy dissipation mechanism involving lubricant action is also present in the tribosystem. In this case, the rate

of entropy dissipation due to lubrication is taken as a certain portion of the total frictional energy dS_i as Equation (3):

$$\frac{dS_f}{dt} = \phi \frac{dS_i}{dt} \quad (3)$$

where, dS_f is the decrease in entropy due to lubricant action, and ϕ is the dissipated portion of the total frictional energy due to the lubricant action. On the other hand, when the tribosystem operates at a stationary state with negligible heat loss to surrounding and insignificant wear particle formation, the entropy generation due to frictional sliding (dS_i/dt) is equal to the entropy dissipation due to wearing process (dS_w/dt) and lubrication (dS_f/dt). As such, equating Equation (1) with Equation (2) and (3) gives a simple equation correlating the friction and the wear of a tribological system [Equation (4)]:

$$k\mathrm{w} = \frac{\mu^2}{cU_w} \quad (4)$$

where, c is the physical characterisation parameter of the tribosystem [Equation(5)]:

$$c = 2A_c \gamma b T w^{-1} v^{-1} \quad (5)$$

and U_w is the dissipative coefficient of the tribosystem [Equation (6)]:

$$U_w = U(1 - \phi)^{-1} \quad (6)$$

In this expression, the parameter c can be calculated based on the physical property of the tribosystem and the operating conditions; whereas U_w is the proportionality constant between the entropy dissipation capability of the lubrication and that of the wear. In reality, both U and ϕ are difficult to measure since they are interfacial properties. Therefore, for simplicity, these parameters are lumped together as U_w to denote the tendency of the tribosystem to cause wear.

Model Parameters Calculation

The use of the friction-wear correlation in Equation (4) to study the Four-ball EP and AW test results of the 36 lubricant samples requires the calculation of the related model parameters. Knowing the distance from the centre of the contact surfaces of the underlying balls to the axis of rotation, x is about 3.67 mm according to the machine specification, the sliding speed, v (ms^{-1}) can be calculated as Equation (7):

$$v = 2\pi w x / 60{,}000 \quad (7)$$

where ω is the rotational speed of the top ball (1760 rpm for the EP test and 1,200 rpm for the AW test). For a given machine loading, L (kg), few contact parameters can be determined (Czichos & Kirschke, 1972; Sethuramiah, 2003).

The normal load on one bottom ball (kg). [Equation(8)]:

$$L_N = 0.408L \quad (8)$$

The contact diameter between the top ball and the bottom ball (mm) [Equation(9)]:

$$d_H = 0.0873L^{1/3} \quad (9)$$

The contact area between the top ball and the bottom ball (mm^2) [Equation(10)]:

$$A_c = \pi d_H^{\,2}/4 \quad (10)$$

In some machines, the friction data is reported as friction torque, F_t (kg-mm). To convert it to friction coefficient, the following formula from IP 239 (2014) is used [Equation (11)].

$$\mu = 0.22248F_T / L \quad (11)$$

In practice, the average wear scar diameter of the bottom balls, d_w (mm) is measured and reported. Based on works (I-Ming, 1962; Sethuramiah, 2003; Wright et al., 1989), d_w can be used to calculate the wear volume of one bottom ball (mm^3) [Equation(12)],

$$V_w = 1.55 \times 10^{-2} \mathrm{d_w}^4 - 1.07 \times 10^{-5} L d_w \quad (12)$$

and the specific wear rate ($mm^3\ N^{-1}\ m^{-1}$)

$$k_w = V_w / (9.81 L_N v t) \quad (13)$$

where, t is the sliding duration (10 s for the EP test and 3,600 s for the AW test). On the other hand, the surface energy, γ of the AISI 52100 steel ball is about 1.95 J m^{-2} based on Fe as in (Inman & Tipler, 1963). For EP tests, the ratio of worn surface area to worn volume, b, is set to 18 mm^{-1}, while for AW tests, it is set to 322 mm^{-1}. The calculated model parameters, along with the experimental data for the 36 samples in the EP and AW tests, are presented in *Table 2* and *3*, respectively.

TABLE 2. THE MODEL PARAMETERS FOR THE FOUR-BALL EP TEST

Sample	Load, L (kg) [a]	Wear scar diameter, d_w (mm) [b]	Average frictional torque, F_t (kg mm)	Friction coefficient, μ	Specific wear rate, k_w ($mm^3\ N^{-1}\ m^{-1}$)	Physical characterisation parameter, c (NKW^{-1})	Dissipative coefficient, U_w ($W\ m^{-2}\ K^{-1}$)
M	80	2.52	105.10	0.292	2.88E-04	0.011	2.80E+13
	100	2.62	118.46	0.264	2.70E-04	0.010	2.60E+13
	126	4.00	456.98	0.807	1.16E-03	0.009	6.10E+13
M + A1	80	2.74	113.80	0.316	4.01E-04	0.011	2.30E+13
	100	2.74	134.88	0.300	3.23E-04	0.010	2.80E+13
	126	4.00	435.02	0.768	1.16E-03	0.009	5.50E+13
M + A2	80	0.42	31.60	0.088	5.67E-08	0.011	1.30E+16
	100	2.44	94.62	0.211	2.03E-04	0.010	2.20E+13
	126	4.00	428.70	0.757	1.16E-03	0.009	5.30E+13
M + A3	80	0.42	30.83	0.086	5.67E-08	0.011	1.20E+16
	100	0.46	27.59	0.061	7.46E-08	0.010	5.10E+15
	126	0.50	42.40	0.075	8.64E-08	0.009	7.00E+15
	160	0.54	48.09	0.067	9.09E-08	0.009	5.80E+15
	200	0.61	54.93	0.061	1.49E-07	0.008	3.20E+15
	250	4.00	63.77	0.057	1.30E-03 [c]	0.007	3.40E+11
M + A1 + A3	160	0.54	45.72	0.064	9.09E-08	0.009	5.20E+15
	200	0.59	48.66	0.054	1.14E-07	0.008	3.20E+15
	250	4.00	325.18	0.289	5.85E-03 [c]	0.007	1.90E+12
M + A2 + A3	160	0.54	39.92	0.056	9.09E-08	0.009	4.00E+15
	200	0.59	55.90	0.062	1.14E-07	0.008	4.30E+15
	250	4.00	59.93	0.053	1.67E-03 [c]	0.007	2.30E+11
M80 + V20	80	2.14	104.12	0.290	1.48E-04	0.011	5.30E+13
	100	2.31	71.41	0.159	1.62E-04	0.010	1.60E+13
	126	4.00	410.95	0.726	1.16E-03	0.009	4.90E+13
M80 + V20 + A1	80	2.41	86.14	0.240	2.39E-04	0.011	2.20E+13
	100	2.51	115.14	0.256	2.28E-04	0.010	2.90E+13
	126	4.00	409.09	0.722	1.16E-03	0.009	4.90E+13
M80 + V20 + A2	80	2.15	80.78	0.225	1.52E-04	0.011	3.10E+13
	100	2.54	81.14	0.181	2.39E-04	0.010	1.40E+13
	126	4.00	410.65	0.725	1.16E-03	0.009	4.90E+13
M80 + V20 + A3	80	2.33	111.86	0.311	2.12E-04	0.011	4.30E+13
	100	2.48	116.07	0.258	2.17E-04	0.010	3.10E+13
	126	4.00	409.60	0.723	1.16E-03	0.009	4.90E+13
M80 + V20 + A1 + A3	80	2.44	99.44	0.277	2.54E-04	0.011	2.80E+13
	100	2.91	133.81	0.298	4.10E-04	0.010	2.20E+13
	126	4.00	414.05	0.731	1.16E-03	0.009	5.00E+13
M80 + V20 + A2 + A3	80	2.28	109.53	0.305	1.93E-04	0.011	4.50E+13
	100	2.75	127.09	0.283	3.28E-04	0.010	2.40E+13
	126	4.00	419.47	0.741	1.16E-03	0.009	5.10E+13

TABLE 2. THE MODEL PARAMETERS FOR THE FOUR-BALL EP TEST (continued)

Sample	Load, L (kg) [a]	Wear scar diameter, d_w (mm) [b]	Average frictional torque, F_t (kg mm)	Friction coefficient, μ	Specific wear rate, k_w ($mm^3\ N^{-1}\ m^{-1}$)	Physical characterisation parameter, c (NKW^{-1})	Dissipative coefficient, U_w ($W\ m^{-2}\ K^{-1}$)
M60 + V40	80	2.51	96.61	0.269	2.81E-04	0.011	2.40E+13
	100	2.79	94.38	0.210	3.45E-04	0.010	1.30E+13
	126	4.00	438.51	0.774	1.16E-03	0.009	5.60E+13
M60 + V40 + A1	80	2.41	80.73	0.225	2.41E-04	0.011	1.90E+13
	100	2.45	70.64	0.157	2.07E-04	0.010	1.20E+13
	126	4.00	387.77	0.685	1.16E-03	0.009	4.40E+13
M60 + V40 + A2	80	2.42	101.28	0.282	2.45E-04	0.011	3.00E+13
	100	2.72	95.73	0.213	3.12E-04	0.010	1.50E+13
	126	4.00	413.17	0.730	1.16E-03	0.009	5.00E+13
M60 + V40 + A3	80	2.11	90.63	0.252	1.41E-04	0.011	4.20E+13
	100	2.26	77.10	0.172	1.49E-04	0.010	2.00E+13
	126	4.00	413.35	0.730	1.16E-03	0.009	5.00E+13
M60 + V40 + A1 + A3	80	2.04	93.87	0.261	1.23E-04	0.011	5.20E+13
	100	2.76	146.97	0.327	3.30E-04	0.010	3.20E+13
	126	4.00	409.13	0.722	1.16E-03	0.009	4.90E+13
M60 + V40 + A2 + A3	80	1.46	51.62	0.144	3.20E-05	0.011	6.00E+13
	100	2.68	116.53	0.259	2.95E-04	0.010	2.30E+13
	126	4.00	429.57	0.759	1.16E-03	0.009	5.40E+13
M40 + V60	80	2.38	80.16	0.223	2.28E-04	0.011	2.00E+13
	100	2.20	63.11	0.140	1.34E-04	0.010	1.50E+13
	126	4.00	383.28	0.677	1.16E-03	0.009	4.30E+13
M40 + V60 + A1	80	0.82	27.78	0.077	2.92E-06	0.011	1.90E+14
	100	2.38	67.94	0.151	1.84E-04	0.010	1.20E+13
	126	4.00	390.72	0.690	1.16E-03	0.009	4.40E+13
M40 + V60 + A2	80	0.70	40.06	0.111	1.41E-06	0.011	8.20E+14
	100	2.48	79.51	0.177	2.16E-04	0.010	1.50E+13
	126	4.00	401.58	0.709	1.16E-03	0.009	4.70E+13
M40 + V60 + A3	80	2.48	102.96	0.286	2.68E-04	0.011	2.80E+13
	100	2.60	83.28	0.185	2.62E-04	0.010	1.30E+13
	126	4.00	367.74	0.649	1.16E-03	0.009	3.90E+13
M40 + V60 + A1 + A3	80	2.47	93.00	0.259	2.63E-04	0.011	2.40E+13
	100	2.91	105.27	0.234	4.10E-04	0.010	1.30E+13
	126	4.00	394.04	0.696	1.16E-03	0.009	4.50E+13
M40 + V60 + A2 + A3	80	2.27	115.42	0.321	1.91E-04	0.011	5.00E+13
	100	3.39	114.22	0.254	7.59E-04	0.010	8.50E+12
	126	4.00	388.33	0.686	1.16E-03	0.009	4.40E+13
M20 + V80	80	1.75	53.57	0.149	6.59E-05	0.011	3.10E+13
	100	2.22	59.96	0.133	1.38E-04	0.010	1.30E+13
	126	4.00	389.31	0.687	1.16E-03	0.009	4.40E+13

TABLE 2. THE MODEL PARAMETERS FOR THE FOUR-BALL EP TEST (continued)

Sample	Load, L (kg) [a]	Wear scar diameter, d_w (mm) [b]	Average frictional torque, F_t (kg mm)	Friction coefficient, μ	Specific wear rate, k_w ($mm^3\ N^{-1}\ m^{-1}$)	Physical characterisation parameter, c (NKW^{-1})	Dissipative coefficient, U_w ($W\ m^{-2}\ K^{-1}$)
M20 + V80 + A1	80	2.33	91.83	0.255	2.12E-04	0.011	2.90E+13
	100	2.37	69.37	0.154	1.79E-04	0.010	1.30E+13
	126	4.00	390.11	0.689	1.16E-03	0.009	4.40E+13
M20 + V80 + A2	80	2.25	74.41	0.207	1.82E-04	0.011	2.20E+13
	100	2.37	88.03	0.196	1.79E-04	0.010	2.10E+13
	126	4.00	435.45	0.769	1.16E-03	0.009	5.50E+13
M20 + V80 + A3	80	2.23	80.35	0.223	1.77E-04	0.011	2.60E+13
	100	2.60	73.76	0.164	2.60E-04	0.010	1.00E+13
	126	4.00	288.39	0.509	1.16E-03	0.009	2.40E+13
M20 + V80 + A1 + A3	80	2.49	79.51	0.221	2.75E-04	0.011	1.70E+13
	100	2.51	97.26	0.216	2.26E-04	0.010	2.10E+13
	126	4.00	377.31	0.666	1.16E-03	0.009	4.10E+13
M20 + V80 + A2 + A3	80	2.38	78.95	0.220	2.30E-04	0.011	1.90E+13
	100	2.35	82.84	0.184	1.73E-04	0.010	2.00E+13
	126	4.00	423.27	0.747	1.16E-03	0.009	5.20E+13
V	80	1.89	42.63	0.119	9.12E-05	0.011	1.40E+13
	100	2.32	50.73	0.113	1.64E-04	0.010	7.80E+12
	126	4.00	356.27	0.629	1.16E-03	0.009	3.70E+13
V + A1	80	1.87	57.74	0.161	8.66E-05	0.011	2.80E+13
	100	2.63	68.30	0.152	2.73E-04	0.010	8.50E+12
	126	4.00	288.94	0.510	1.16E-03	0.009	2.40E+13
V + A2	80	2.32	71.59	0.199	2.08E-04	0.011	1.80E+13
	100	2.66	71.45	0.159	2.84E-04	0.010	8.90E+12
	126	4.00	370.08	0.653	1.16E-03	0.009	4.00E+13
V + A3	80	0.42	24.88	0.069	5.67E-08	0.011	7.80E+15
	126	0.50	37.85	0.067	8.64E-08	0.009	5.60E+15
	160	0.54	39.83	0.055	9.09E-08	0.009	4.00E+15
	200	4.00	266.06	0.296	7.32E-03 [c]	0.008	1.50E+12
V + A1 + A3	160	0.54	40.88	0.057	9.09E-08	0.009	4.20E+15
	200	4.00	56.88	0.063	7.32E-04	0.008	6.90E+11
V + A2 + A3	160	0.54	41.33	0.057	9.09E-08	0.009	4.30E+15
	200	0.74	43.69	0.049	5.58E-07	0.008	5.30E+14
	250	4.00	331.29	0.295	5.85E-03 [c]	0.007	2.00E+12

Note: [a] - The weld point corresponds to the heaviest load used in the test of each oil sample; [b] - Measured using the DUCOM imaging device for the non-welded ball. In the case of the welded ball, the wear scar diameter is treated as 4 mm and [c] - Calculated based on shorter sliding time since the ball welded before test duration: M + A3 (sliding time of 4.5 s); M + A1 + A3 (1.0 s); M + A2+ A3 (3.5 s); V + A3 (1.0 s); V + A2 + A3 (1.0 s).

TABLE 3. THE MODEL PARAMETERS FOR THE FOUR-BALL AW TEST

Sample	Load, L (kg) [a]	Wear scar diameter, d_w (mm) [b]	Average frictional torque, F_t (kg mm)	Friction coefficient, μ	Specific wear rate, k_w ($mm^3\ N^{-1}\ m^{-1}$)	Physical characterisation parameter, c (NKW^{-1})	Dissipative coefficient, U_w ($W\ m^{-2}\ K^{-1}$)
M	40	0.73	14.03	0.078	1.58E-08	0.355	1.1E+15
M + A1	40	0.54	21.25	0.118	4.06E-09	0.355	9.7E+15
M + A2	40	0.51	25.78	0.143	3.21E-09	0.355	1.8E+16
M + A3	40	0.64	23.12	0.129	9.00E-09	0.355	5.2E+15
M + A1 + A3	40	0.52	23.64	0.131	3.33E-09	0.355	1.5E+16
M + A2 + A3	40	0.60	14.59	0.081	6.55E-09	0.355	2.8E+15
M80 + V20	40	0.51	25.85	0.144	3.10E-09	0.355	1.9E+16
M80 + V20 + A1	40	0.58	22.88	0.127	5.84E-09	0.355	7.8E+15
M80 + V20 + A2	40	0.54	45.97	0.256	4.06E-09	0.355	4.5E+16
M80 + V20 + A3	40	0.54	26.16	0.145	3.95E-09	0.355	1.5E+16
M80 + V20 + A1 + A3	40	0.42	26.26	0.146	1.19E-09	0.355	5.1E+16
M80 + V20 + A2 + A3	40	0.40	30.58	0.170	8.49E-10	0.355	9.6E+16
M60 + V40	40	0.51	26.28	0.146	3.21E-09	0.355	1.9E+16
M60 + V40 + A1	40	0.60	12.54	0.070	6.74E-09	0.355	2.0E+15
M60 + V40 + A2	40	0.56	25.40	0.141	4.91E-09	0.355	1.1E+16
M60 + V40 + A3	40	0.55	20.14	0.112	4.34E-09	0.355	8.1E+15
M60 + V40 + A1 + A3	40	0.54	17.77	0.099	4.20E-09	0.355	6.5E+15
M60 + V40 + A2 + A3	40	0.55	14.27	0.079	4.49E-09	0.355	3.9E+15
M40 + V60	40	0.60	23.75	0.132	6.74E-09	0.355	7.3E+15
M40 + V60 + A1	40	0.60	19.23	0.107	6.74E-09	0.355	4.8E+15
M40 + V60 + A2	40	0.58	27.52	0.153	5.54E-09	0.355	1.2E+16
M40 + V60 + A3	40	0.39	36.65	0.204	7.21E-10	0.355	1.6E+17
M40 + V60 + A1 + A3	40	0.34	13.31	0.074	2.63E-10	0.355	5.9E+16
M40 + V60 + A2 + A3	40	0.54	27.52	0.153	4.06E-09	0.355	1.6E+16
M20 + V80	40	0.61	27.56	0.153	7.15E-09	0.355	9.2E+15
M20 + V80 + A1	40	0.61	22.53	0.125	6.94E-09	0.355	6.4E+15
M20 + V80 + A2	40	0.63	27.69	0.154	7.95E-09	0.355	8.4E+15
M20 + V80 + A3	40	0.44	25.43	0.141	1.44E-09	0.355	3.9E+16
M20 + V80 + A1 + A3	40	0.39	21.36	0.119	7.59E-10	0.355	5.2E+16
M20 + V80 + A2 + A3	40	0.39	7.91	0.044	7.59E-10	0.355	7.2E+15
V	40	0.63	16.61	0.092	8.35E-09	0.355	2.9E+15
V + A1	40	0.55	20.74	0.115	4.45E-09	0.355	8.4E+15
V + A2	40	0.69	24.17	0.134	1.18E-08	0.355	4.3E+15
V + A3	40	0.66	21.57	0.120	9.75E-09	0.355	4.2E+15
V + A1 + A3	40	0.57	23.30	0.130	5.20E-09	0.355	9.1E+15
V + A2 + A3	40	0.66	22.34	0.124	9.75E-09	0.355	4.5E+15

RESULTS AND DISCUSSION

Mapping of Friction-wear Relationships in Four-ball Lubrications

The friction and the wear behaviours of a lubricated tribosystem are interrelated in such a way that the wear increases with the friction during sliding activity. The friction-wear relationship can be categorised and mapped into certain performance regions according to the thermodynamic framework as illustrated in *Figure 1*. The figure captures the friction-wear behaviours of lubrication in a Four-ball tribo-tester running at various conditions from mild-wear condition (e.g., 40–60 kg load) up to moderate/severe wear condition (e.g., 80–126 kg load) and finally weld point (e.g., 126–250 kg load). A glance at the figure clearly shows that both the mineral-based and vegetable-based lubrication behave similarly in the EP and AW tests, whereby the wear generally increases with sliding friction. As shown in *Figure 1*, one important parameter governing the performance regions is the dissipative coefficient U_w, which simply denotes the tendency of the tribosystem to cause wear at a specific sliding condition. For instance, the high value of U_w represents less tendency to cause wear in the tribosystem at the specific sliding conditions (i.e., load and speed). In other words, the change of U_w corresponds to the change in wear conditions of the triboparts and also that in the sliding conditions. At mild wear conditions (k_w = 1 × 10^{-8} to 1 × 10^{-6} mm^3 N^{-1} m^{-1}) such as in the AW test (i.e., 40 kg load) and in low load EP test (i.e., < 63 kg load), the tribosystem was able to dissipate the frictional energy efficiently without inducing much wear. Within the mild wear region, the friction-wear relationship is bounded by U_w of the order of 10^{15} to 10^{17} W m^{-2} K^{-1}. Following that, when the load in the EP test increased further, the wear of the triboparts reached the severe wear region (k_w> 1 × 10^{-6} mm^3 N^{-1} m^{-1}). This wear region is narrowly governed by U_w of the order of 10^{13} to 10^{14} W m^{-2} K^{-1}. Up to this point, the friction-wear relationship of the lubrication is mainly influenced by the base oil portion of the lubrication regardless of mineral-based or vegetable-based. Further, increase in load may result in welding of triboparts unless tribo-performance additives in the lubrications are present and active. The result in *Figure 1* shows that lubrications with active tribo-performance additives are characterised by U_w in the order of 10^{11} to 10^{13} W m^{-2} K^{-1}. Because of this region, it is interesting to note that there are two additive mechanisms in action at the extreme sliding conditions: one generated higher friction (U_w in the order of 10^{12} to 10^{13}) and the other one produced lower friction (U_w in the order of 10^{11} to 10^{12}). From the model perspective, the tribo-performance (EP or AW) additives provide an additional entropy dissipation mechanism on top of the base oil mechanism to balance out with the friction entropy generation from the sliding condition, especially at load beyond the weld point of the base oil.

In summary, the U_w parameter represents the tendency of the tribosystem to cause wear (Chan et al., 2020). Indirectly, it also indicates the state of the lubrication mechanism in action during the sliding activity. *Table 4* tabulates the characteristics of the lubrications at various U_w values and their significance according to the modelling framework. In practice, the classification of the magnitude order of the dissipative coefficient U_w determines the lubrication mechanism in action, which is beneficial to the lubricant formulation and the selection of suitable additives. In the next section, the individual effects of additive A1, A2 and A3 based on U_w parameter are assessed.

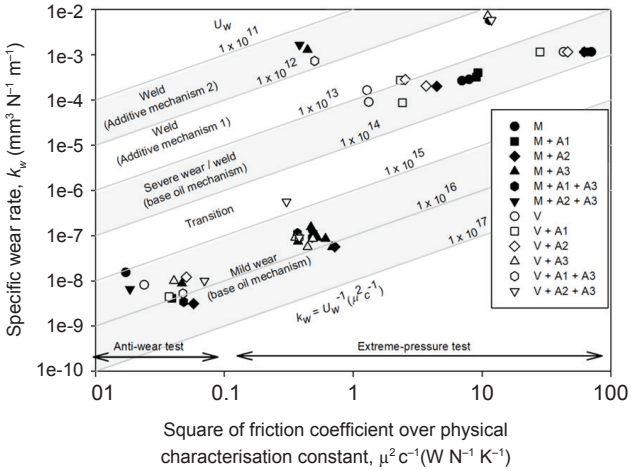

Figure 1. Friction-wear relationship of M and V with additives (A1, A2 and A3) in the anti-wear and extreme pressure tests. The highlighted regions are bounded by a certain range of dissipative coefficient U_w.

TABLE 4. THE DISSIPATIVE COEFFICIENT U_W AND ITS ENTROPY DISSIPATION MECHANISM

No.	The dissipative coefficient U_w (W m^{-2} K^{-1})	Wear condition	Possible lubrication mechanisms	Significance and implication
1	1×10^{15} to 1×10^{17}	Mild wear	BASE mechanism: Lubricant film thickness; viscosity effect; and lubrication regimes such as mixed, boundary lubrication	Both mineral-based and vegetable-based lubrications behave similarly
2	1×10^{14} to 1×10^{15}	Transition	BASE mechanism	The lubrication cannot be sustained in this unstable region
3	1×10^{13} to 1×10^{14}	Severe	BASE mechanism	Both mineral-based and vegetable-based lubrications behave similarly. (Weld point = 126 kg)
4	1×10^{12} to 1×10^{13}	Weld point	EP additive mechanism 1: Formation of a protective layer	The lubrication has a high weld point (> 126 kg). It generated higher friction
5	1×10^{11} to 1×10^{12}	Weld point	EP additive mechanism 2: Formation of a protective layer	The lubrication has a high weld point (> 126 kg). It generated lower friction

Additive Synergy to Enhance EP and AW Performances

The synergy of the additive A1, A2 and A3 in the mineral-based and vegetable-based lubrications in the EP test and the AW test were assessed experimentally. In view of the tribological additives, A1 and A2 are AW additives, whereas A3 is an EP additive. A glance at *Figure 2* shows that the additive synergy in the mineral-based and vegetable-based lubrication was distinct. Certain combinations of additives worked well in certain BASE as they offered greater advantages than the individual effect of the additives. In the case of mineral oil lubrication, *Figure 2a* illustrates that the additive A1 and A2 were able to reduce the friction of the contact slightly without changing the weld point of the lubrication in the EP test, while the additive A3 was able to increase the weld point of the mineral oil from 126–250 kg. These additives offer no synergistic advantage in terms of weld point when they are paired with A3 in the mineral oil formulation. From a conventional viewpoint, the lubrication M + A1 + A3 seemed to be antagonistic because of poorer frictional performance than M + A3 in the EP test. In *Figure 2b*, the additive A2 worked better than the additive A1 in terms of wear minimisation effect in the AW test, despite the formed incurring a higher friction coefficient. The EP additive A3 also gave a slight wear minimisation effect. In terms of additive synergy, in this case, no significant effect was observed in the mineral-based lubrication with any additive combination. On the other hand, looking at the effect of the additives in V lubrication in the EP test as in *Figure 2c*, the EP additive A3 enhanced the weld point of the lubrication to 200 kg. When the additive A2 was coupled with the additive A3, the weld point was boosted further to 250 kg. However, on individual additive effect, the additive A1 provided a positive effect in terms of frictional performance, while the additive A2 gave no significant positive effect. With regards to the additive performance in AW test, there is no conclusive remark that can be drawn based on the result in *Figure 2d*. This is because the result of the wear scar diameter and also the friction coefficient were span narrowly and they are not significantly different than each other. In this assessment of additive synergy, some interactions are difficult to identify and confirm, based on merely experimental parameters. A thorough and simplistic assessment using a modelling approach can be employed and will be demonstrated in the following section. To maintain a fair comparison, both the assessments through the experimental parameters and the modelling approach must be based on an identical dataset. Since the modelling approach prioritises the identification of trends over the precision of individual data points, incorporating error bars or data repetition in *Figure 2* is unnecessary for this comparison study.

Assessment of Lubricant Formulations via the Modelling Approach

This study demonstrated the assessment of the tribological performance of various lubricant formulations in the AW and the EP test based on the dissipative coefficient U_w. In this assessment, the lubrication with a higher value of U_w has better tribological performance in general. This is because it has a higher dissipation rate of frictional entropy and hence lesser tendency to cause wear. For fair assessment, the comparison between two lubrications must be made at the same operating conditions, especially at the same load and sliding speed. The modelling results presented in *Figure 3* illustrated the effect of blending the V into the M from 0%–100% in five formulations (BASE; BASE + A1; BASE + A2; BASE + A3; BASE + A1 + A3;

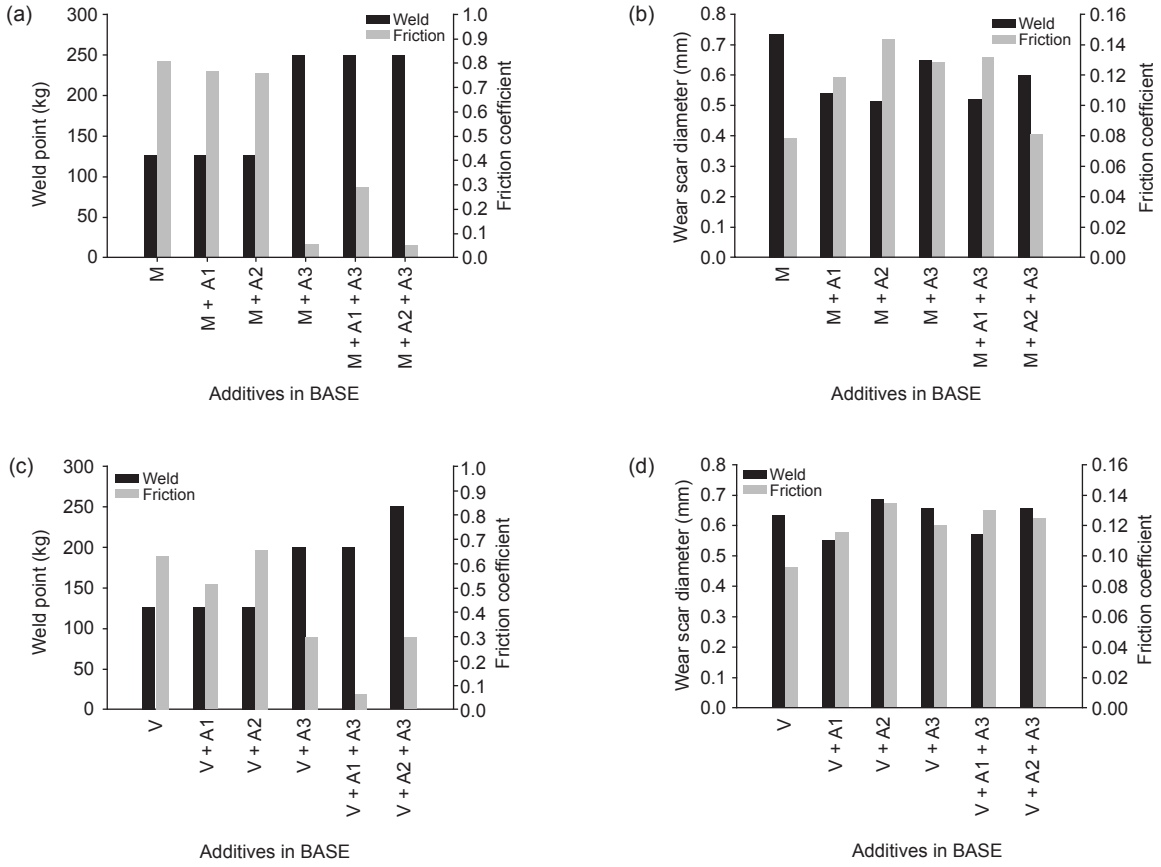

Figure 2. Tribological results of mineral-based lubrications in (a) the EP test and (b) the AW test; while vegetable-based lubrications in (c) the EP test and (d) the AW test.

BASE + A2 + A3) during the AW test. From the results, incorporating V in all five formulations was found to be beneficial probably due to the advantages of the oil in lubricity and friction performances as suggested in work (Reeves et al., 2015). The optimum BASE compositions for each of the lubricant formulations based on highest U_w value are: BASE (M80 + V20 and M60 + V40); BASE + A1 (M and V); BASE + A2 (M80 + V20); BASE + A3 (M40 + V60); BASE + A1 + A3 (M40 + V60) and BASE + A2 + A3 (M80 + V20). The above results suggest that the additive A1 and A3 have affinity to both the M and V, whereas the additive A2 favours mineral-rich formulations.

Overall, the formulation BASE + A3 (M40 + V60) gave the best AW performance from the thermodynamic perspective. Nevertheless, it generated 0.39 mm wear scar diameter, which is slightly larger than the 0.34 mm wear scar diameter from the formulation of BASE + A1 + A3 (M40 + V60). Because of that, the former is considered to be the optimum formulation from the thermodynamic point of view, whereas the latter is the best according to the experimental results. In practice, if few formulations achieved similar experimental results, the modelling approach emphasising the U_w parameter can be a great help in identifying the better formulation. This can be demonstrated in the case of the EP test in this study.

On the other hand, the modelling result of the lubrications in the EP test is plotted in *Figure 4*. Note that the effect of blending the V into the M from 0%–100% is not illustrated in the figure because they did not exhibit significant effects. The weld points of the blended oils, even in the formulations involving additives, were still at 126 kg as tabulated in *Table 2*. Based on the modelling results of the lubrication performances at the weld point of 250 kg, the lubrication V + A2 + A3 performed slightly better than the lubrication M + A1 + A3. However, in the load below the weld point such as at 200 kg, the lubrication M + A2 + A3 outperformed the lubrications V + A2 + A3 and M + A1 + A3. This observation suggests that lubricant with a higher weld point may not necessarily be the best choice for the application that requires a lower weld point lubricant. In this modelling approach, the U_w values of the lubrications serve as an additional parameter on top of the weld point, to assess and select the best lubrication formulations out from the list of lubrications that passed the EP test.

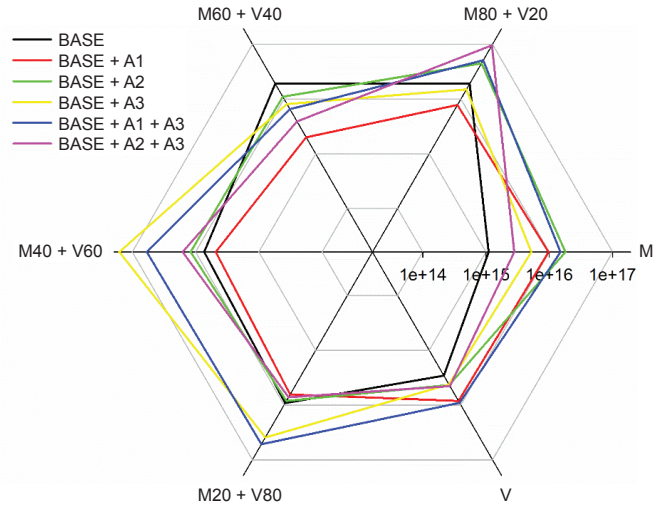

Figure 3. The dissipative coefficient U_w *of lubrications under the AW test for lubricant samples at different base oil compositions and additives formulations.*

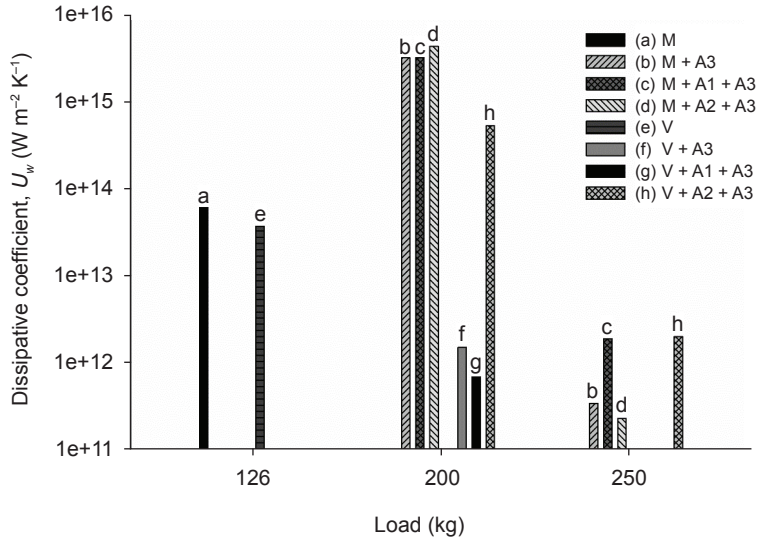

Figure 4. The dissipative coefficient U_w *of lubrications under the EP test for lubricant samples at different base oils and additives formulations.*

The Model Implication and Applications

In practice, the conventional tribological data such as friction coefficient and wear scar diameter can only be used in comparing the relative performance of two or more lubricants. If the tribological data obtained from the comparison is similar or not significantly different, no conclusive remark can be drawn. To overcome this problem, the modelling approach introduced in this work helps the lubrication assessment from the thermodynamic perspective. This modelling approach utilises U_w parameter to gauge the effectiveness of the lubrication in minimising wear and to sustain the activity of the tribosystem. One can select the best lubricant or lubricant composition based on the magnitude of U_w, in which the larger the magnitude of U_w, the better the lubrication and its mechanism to minimise wear at the designated operating condition. Despite the fact that U_w is not a physical parameter that can be measured experimentally, it is useful in the assessment and interpretation of lubrication performance. In terms of reliability, the friction-wear relationship and the performance region bounded by the specific ranges of U_w (*Table 4*) are very consistent and reliable across different lubricant samples, such as M and V in this work and also other synthetic oils in the previous work (Chan et al., 2020).

TABLE 5. RANKING OF THE LUBRICANT FORMULATIONS IN THE AW AND EP TESTS

Item	Traditional approach[a]	Modelling approach[b]
Anti-wear test	M40 + V60 + A1 + A3 (0.34 mm)	M40 + V60 + A3 (1.6E+17 W m^{-2} K^{-1})
	M40 + V60 + A3 (0.39 mm)	M80 + V20 + A2 + A3 (9.6E+16 W m^{-2} K^{-1})
	M20 + V80 + A1 + A3 (0.39 mm)	M40 + V60 + A1 + A3 (5.9E+16 W m^{-2} K^{-1})
	M20 + V80 + A2 + A3 (0.39 mm)	M20 + V80 + A1 + A3 (5.2E+16 W m^{-2} K^{-1})
	M80 + V20 + A2 + A3 (0.40 mm)	M80 + V20 + A1 + A3 (5.1E+16 W m^{-2} K^{-1})
Extreme pressure test	M + A3[c] (250 kg)	V + A2 + A3 (2.0E+12 W m^{-2} K^{-1})
	M + A1 + A3[c] (250 kg)	M + A1 + A3 (1.9E+12 W m^{-2} K^{-1})
	M + A2 + A3[c] (250 kg)	M + A3 (3.4E+11 W m^{-2} K^{-1})
	V + A2 + A3[c] (250 kg)	M + A2 + A3 (2.3E+11 W m^{-2} K^{-1})

Note: [a] - The value in parentheses is wear scar diameter (AW test) and weld point (EP test); [b] - The value in parentheses is the dissipative coefficient U_w; [c] - Unable to determine the ranking of lubricant formulation.

In this study, the top lubricant formulations in the AW test and also the EP test are selected and listed in *Table 5*. The selection is based on the traditional approach (i.e., tribological data) and the modelling approach (i.e., dissipative coefficient U_w). As can be seen in the table, the ranking of lubricant formulations based on the modelling approach is different from the traditional approach. In view of the AW test, the best-performing lubricants gave wear scar diameter ranged from 0.34–0.40 mm and there are three lubricants which scored similar results (0.39 mm). In this case, it is not possible to rank the lubrication performance according to wear scar diameter. However, ranking of the lubrication performance is possible based on their dissipative coefficients. On the other hand, a similar issue was found in the EP test as well. The best lubricant formulation is difficult to determine based on weld point alone since all scored 250 kg. With the use of the dissipative coefficient, the ranking of lubrication performance can be conducted. In this study, the modelling approach concluded that M40 + V60 + A3 lubricant is the best formulation for the anti-wear test, while V + A2 + A3 is the best in the extreme-pressure test.

CONCLUSION

This study has pioneered a comprehensive modelling approach designed to elevate the assessment of lubrication effectiveness within the realms of the ASTM D2783 EP and ASTM D4172 AW tests. The modelling approach serves to determine the optimal high-performance lubrication and synergistic additive combination, even in scenarios where the evaluated lubricants yield similar outcomes in tribological assessments. This is possible through the determination of the dissipative coefficient U_w of the lubrication. U_w operates as a reliable assessment parameter, offering insight into the lubrication capability to minimise wear and sustain tribological operations effectively. From the thermodynamic viewpoint, a lubricant boasting a higher U_w value demonstrates heightened efficiency in quelling the accumulation of frictional entropy inherent to a lubricated tribological system. As a result, this attribute reduces the tendency and intensity of wear within the system. Expanding beyond the realms of lubrication assessment, the dissipative coefficient U_w also finds use in constructing the friction-wear relationship for lubrication. This mapping of lubrication performance proves invaluable for the design of lubricant formulations. It serves as a tool to investigate the synergistic interactions between base oils and additives, to gauge the lubrication efficacy across diverse sliding conditions and to facilitate comparative analyses between two distinct lubricants. The prowess of this modelling approach finds substantial validation within a comprehensive case study involving 36 lubricant samples, comprising M, V and their various blends, supplemented by an array of tribological additives.

ACKNOWLEDGEMENT

The authors are thankful for the financial assistance provided by the Malaysian Palm Oil Board.

REFERENCES

Abdel-Aal, H. A. (2010). Influence of frictional energy dissipation on wear regime transition in dry tribo-systems. *International Journal of Materials and Product Technology*, *38*(1), 78–92. https://doi.org/10.1504/ijmpt.2010.031897

Aldana, P. U., Dassenoy, F., Vacher, B., Le Mogne, T., & Thiebaut, B. (2016). WS_2 nanoparticles anti-wear and friction reducing properties on rough surfaces in the presence of ZDDP additive. *Tribology International*, *102*, 213–221. https://doi.org/10.1016/j.triboint.2016.05.042

Allmaier, H., Priestner, C., Reich, F. M., Priebsch, H. H., Forstner, C., & Novotny-Farkas, F. (2011). Predicting friction reliably and accurately in journal bearings – The importance of extensive oil-models. *Tribology International*, *48*, 93–101. https://doi.org/10.1016/j.triboint.2011.11.009

Amiri, M., & Khonsari, M. M. (2010). On the thermodynamics of friction and wear – A review. *Entropy*, *12*(5), 1021–1049. https://doi.org/10.3390/e12051021

ASTM International. (ASTM). (2019). *Standard test method for measurement of extreme-pressure properties of lubricating fluids (four-ball method)* (ASTM D2783-19).

ASTM International. (ASTM). (2020). *Standard test method for wear preventive characteristics of lubricating fluid (four-ball method)* (ASTM D4172-20).

Banjac, M., Vencl, A., & Otović, S. (2014). Friction and wear processes – Thermodynamic approach. *Tribology in Industry*, *36*(4), 341–347.

Bart, J., Gucciardi, E., & Cavallaro, S. (2013). Formulating lubricating oils. In *Biolubricants* (pp. 351–395). Woodhead Publishing.

Baskar, S., Sriram, G., & Arumugam, S. (2016). The use of D-optimal design for modeling and analyzing the tribological characteristics of journal bearing materials lubricated by nano-based biolubricants. *Tribology Transactions*, *59*(1), 44–54. https://doi.org/10.1080/10402004.2015.1063179

Bosman, R., & Schipper, D. J. (2011). Mild wear prediction of boundary-lubricated contacts. *Tribology Letters*, *42*(2), 169–178. https://doi.org/10.1007/s11249-011-9760-3

Bosman, R., & Schipper, D. J. (2012). Mild wear maps for boundary lubricated contacts. *Wear*, *280–281*, 54–62. https://doi.org/10.1016/j.wear.2012.01.019

Cao, S., Maldonado, S. G., & Mischler, S. (2014). Tribocorrosion of passive metals in the mixed lubrication regime: Theoretical model and application to metal-on-metal artificial hip joints. *Wear*, *324–325*, 55–63. https://doi.org/10.1016/j.wear.2014.12.003

Chan, C. H., Lim, W. H., Yeong, S. K., Kow, K. W., & Ho, Y. K. (2020). A friction-wear correlation for Four-ball extreme pressure lubrication. *Journal of Tribology*, *142*(2), 021702. https://doi.org/10.1115/1.4044879

Chong, W. W. F., & Ng, J. H. (2016). An atomic-scale approach for biodiesel boundary lubricity characterisation. *International Biodeterioration & Biodegradation*, *113*, 34–43. https://doi.org/10.1016/j.ibiod.2016.03.029

Czichos, H., & Kirschke, K. (1972). Investigations into film failure (transition point) of lubricated concentrated contacts. *Wear*, *22*(3), 321–336. https://doi.org/10.1016/0043-1648(72)90392-4

Energy Institute. (2014). *Determination of extreme pressure and anti-wear properties of lubricating fluids and greases - Four ball method (European conditions)* (Standard No. IP 239).

Fox-Rabinovich, G., Veldhuis, S. C., Kovalev, A. I., Wainstein, D. L., Gershman, I. S., Korshunov, S., Shuster, L. S., & Endrino, J. L. (2007). Features of self-organization in ion modified nanocrystalline plasma vapor deposited AlTiN coatings under severe tribological conditions. *Journal of Applied Physics*, *102*(7), 074305. https://doi.org/10.1063/1.2785947

Gan, S., Chen, R. S., Padzil, F. N. M., Moosavi, S., Tarawneh, M. A., Loh, S. K., & Idris, Z. (2023). Potential valorization of oil palm fiber in versatile applications towards sustainability: A review. *Industrial Crops and Products*, *199*, 116763. https://doi.org/10.1016/j.indcrop.2023.116763

Gao, L., Hua, Z., & Hewson, R. (2018). Can a "pre-worn" bearing surface geometry reduce the wear of metal-on-metal hip replacements? – A numerical wear simulation study. *Wear*, *406–407*, 13–21. https://doi.org/10.1016/j.wear.2018.03.010

Gershman, I., Gershman, E., Mironov, A., Fox-Rabinovich, G., & Veldhuis, S. (2016). Application of the self-organization phenomenon in the development of wear resistant materials – A review. *Entropy*, *18*(11), 385. https://doi.org/10.3390/e18110385

Ghaffari, M. A., Zhang, Y., & Xiao, S. (2018). Multiscale modeling and simulation of rolling contact fatigue. *International Journal of Fatigue*, *108*, 9–17. https://doi.org/10.1016/j.ijfatigue.2017.11.005

Ghanbarzadeh, A., Wilson, M., Morina, A., Dowson, D., & Neville, A. (2016). Development of a new mechano-chemical model in boundary lubrication. *Tribology International*, *93*, 573–582. https://doi.org/10.1016/j.triboint.2014.12.018

Godlevskiy, V., & Blinov, O. V. (2016). Computing of the molecular orientation state of the lubrication layer. *Procedia Engineering*, *150*, 584–589. https://doi.org/10.1016/j.proeng.2016.07.046

Hao, L., & Meng, Y. (2015). Numerical prediction of wear process of an initial line contact in mixed lubrication conditions. *Tribology Letters*, *60*, 31. https://doi.org/10.1007/s11249-015-0609-z

Hu, Y., Wang, L., Politis, D., & Masen, M. (2017). Development of an interactive friction model for the prediction of lubricant breakdown behaviour during sliding wear. *Tribology International*, *110*, 370–377. https://doi.org/10.1016/j.triboint.2016.11.005

I-Ming, F. (1962). A new approach in interpreting the four-ball wear results. *Wear*, *5*(4), 275–288. https://doi.org/10.1016/0043-1648(62)90130-8

Inman, M. C., & Tipler, H. R. (1963). Interfacial energy and composition in metals and alloys. *Metallurgical Reviews*, *8*(1), 105–166. https://doi.org/10.1179/mtlr.1963.8.1.105

Lee, C. T., Lee, M. B., Mong, G. R., & Chong, W. W. F. (2022). A bibliometric analysis on the tribological and physicochemical properties of vegetable oil-based bio-lubricants (2010–2021). *Environmental Science and Pollution Research*, *29*, 56215–56248. https://doi.org/10.1007/s11356-022-19746-2

Li, S., & Anisetti, A. (2017). A tribo-dynamic contact fatigue model for spur gear pairs. *International Journal of Fatigue*, *98*, 81–91. https://doi.org/10.1016/j.ijfatigue.2017.01.020

Li, S., Kahraman, A., Anderson, N., & Wedeven, L. (2013). A model to predict scuffing failures of a ball-on-disk contact. *Tribology International*, *60*, 233–245. https://doi.org/10.1016/j.triboint.2012.11.007

Lyashenko, I. A., & Khomenko, A. V. (2012). Thermodynamic theory of two rough surfaces friction in the boundary lubrication mode. *Tribology Letters*, *48*(1), 63–75. https://doi.org/10.1007/s11249-012-9939-2

Mishina, H., & Hase, A. (2013). Wear equation for adhesive wear established through elementary process of wear. *Wear*, *308*(1–2), 186–192. https://doi.org/10.1016/j.wear.2013.06.016

Mukchortov, I., Zadorozhnaya, E., & Polyacko, E. (2017). Transitional friction regime modeling under boundary lubrication conditions. *Procedia Engineering*, *206*, 725–733. https://doi.org/10.1016/j.proeng.2017.10.544

Ouyang, T., Huang, H., Zhang, N., Mo, C., & Chen, N. (2017). A model to predict tribo-dynamic performance of a spur gear pair. *Tribology International*, *116*, 449–459. https://doi.org/10.1016/j.triboint.2017.08.005

Parveez, G. K. A., Rasid, O. A., Ahmad, M. N., Taib, H. M., Bakri, M. A. M., Hafid, S. R. A., Ismail, T. N. M., Loh, S. K., Abdullah, M. O., Zakaria, K., & Idris, Z. (2023). Oil palm economic performance in Malaysia and R&D progress in 2022. *Journal of Oil Palm Research*, *35*(2), 193–216. https://doi.org/10.21894/jopr.2023.0028

Ramalho, A., & Miranda, J. C. (2006). The relationship between wear and dissipated energy in sliding systems. *Wear*, *260*(4–5), 361–367. https://doi.org/10.1016/j.wear.2005.02.121

Reeves, C. J., Menezes, P. L., Jen, T. C., & Lovell, M. R. (2015). The influence of fatty acids on tribological and thermal properties of natural oils as sustainable biolubricants. *Tribology International*, *90*, 123–134. https://doi.org/10.1016/j.triboint.2015.04.021

Ripoll, M. R., Podgornik, B., & Vižintin, J. (2011). Finite element analysis of textured surfaces under reciprocating sliding. *Wear*, *271*(5–6), 952–959. https://doi.org/10.1016/j.wear.2011.04.003

Sethuramiah, A. (Ed.) (2003). *Lubricated wear: Science and technology*. Elsevier.

Simonovic, K., & Kalin, M. (2016). Methodology of a statistical and DOE approach to the prediction of performance in tribology – A DLC boundary-lubrication case study. *Tribology*

International, *101*, 10–24. https://doi.org/10.1016/j.triboint.2016.04.007

Tan, Y., Zhang, L., & Hu, Y. (2014). A wear model of plane sliding pairs based on fatigue contact analysis of asperities. *Tribology Transactions*, *58*(1), 148–157. https://doi.org/10.1080/10402004.2014.956907

Tomala, A., Ripoll, M. R., Gabler, C., Remškar, M., & Kalin, M. (2017). Interactions between MoS_2 nanotubes and conventional additives in model oils. *Tribology International*, *110*, 140–150. https://doi.org/10.1016/j.triboint.2017.01.036

Vakis, A. I., Yastrebov, V. A., Scheibert, J., Nicola, L., Dini, D., Minfray, C., Almqvist, A., Paggi, M., Lee, S., Limbert, G., Molinari, J., Anciaux, G., Aghababaei, R., Restrepo, S. E., Papangelo, A., Cammarata, A., Nicolini, P., Putignano, C., Carbone, G., . . . Ciavarella, M. (2018). Modeling and simulation in tribology across scales: An overview. *Tribology International*, *125*, 169–199. https://doi.org/10.1016/j.triboint.2018.02.005

Weinebeck, A., Kaminski, S., Murrenhoff, H., & Leonhard, K. (2017). A new QSPR-based prediction model for biofuel lubricity. *Tribology International*, *115*, 274–284. https://doi.org/10.1016/j.triboint.2017.05.005

Wright, M. S., Jain, V. K., & Saba, C. S. (1989). Wear rate calculation in the Four-ball wear test. *Wear*, *134*(2), 321–334. https://doi.org/10.1016/0043-1648(89)90134-8

Xiong, S., Sun, J., Xu, Y., & Yan, X. (2015). QSPR models for the prediction of friction coefficient and maximum non-seizure load of lubricants. *Tribology Letters*, *60*(1), 1–8. https://doi.org/10.1007/s11249-015-0590-6

Yang, S., Zhang, D., Wong, J. S., & Cai, M. (2021). Interactions between ZDDP and an oil-soluble ionic liquid additive. *Tribology International*, *158*, 106938. https://doi.org/10.1016/j.triboint.2021.106938

Zhang, J., Liu, S., & Fang, T. (2017). On the prediction of friction coefficient and wear in spiral bevel gears with mixed TEHL. *Tribology International*, *115*, 535–545. https://doi.org/10.1016/j.triboint.2017.06.035

Zhou, C., Hu, B., Qian, X., & Han, X. (2018). A novel prediction method for gear friction coefficients based on a computational inverse technique. *Tribology International*, *127*, 200–208. https://doi.org/10.1016/j.triboint.2018.06.005